

Engineering Notes

ENGINEERING NOTES are short manuscripts describing new developments or important results of a preliminary nature. These Notes cannot exceed 6 manuscript pages and 3 figures; a page of text may be substituted for a figure and vice versa. After informal review by the editors they may be published within a few months of the date of receipt. Style requirements are the same as for regular contributions (see inside back cover).

Collapse Analysis of Cylindrical Composite Panels with Cutouts

T. C. Janisse* and A. N. Palazotto†

Air Force Institute of Technology
Wright-Patterson Air Force Base, Ohio

Introduction

IN the aircraft industry, various studies have been conducted both experimentally and analytically^{1,3} on the buckling of composite panels and plates under axial compression. However, very little information on composite panels with cutouts can be found. There have been studies done on cutout reinforcement in composite shells⁴ and on flat rectangular graphite epoxy plates with either surface damage or cutouts.^{5,6} No studies were found relating the effect of cutouts on curved composite panels.

A nonlinear analysis using the STAGS C 1 computer code has been used herein.⁷ In addition, a study has been made to evaluate the effect of ply layup with two cutout sizes and three different composite panel ply orientations.

Modeling

Panel Properties

This study has modeled a graphite epoxy composite panel as shown in Fig. 1. The ply orientations studied are listed on the top of Fig. 2. A boundary condition has been assumed in which the top of the panel is clamped with only the u degree of freedom (DOF) free and the bottom of the panel is totally clamped with no free DOFs. The vertical sides of the panel are simply supported with u , v , and rotation about x free. The panel is loaded into compression with a controlled distribution load N_x along the top edge. The material properties of each ply are $E_1=20,500$ ksi, $E_2=1300$ ksi, $G_{12}=750$ ksi, and $\nu_{12}=0.335$.

Grid Selection

The first panel modeled has a 2×2 in² opening located in the center of the panel. There are two grid sizes (13×13 and 25×25) with constant spacing that will be used to model this panel. The critical load for nonlinear collapse was computed for both grid sizes. The coarser grid completed its collapse load calculations in only 20% of the CPU time of the finer grid. Since both grid sizes were very close to each other in stiffness with only a 12.5% difference in the collapse load, the coarser grid size has been used, as the phenomenon of

collapse is the important part of this study not the exact numerical comparisons.

A compatibility problem at the junction of elements will arise when modeling a curved panel with flat elements. The 411 element (a rectangular 32 DOF element) in STAGS has been developed specifically so that the displacement compatibility can be incorporated for flat elements meeting at a nonzero angle.⁷

Discussion and Results

A graph of the top edge load vs the top edge displacement is shown in Fig. 2 for the panels with and without cutouts. When considering just the linear bifurcation of the panels, it can be seen that the presence of a cutout greatly reduces the load bearing capability of the panel and its stiffness. The linear bifurcation of the panels shown in Fig. 2 is for a $[0, +45, -45, 90]_s$ ply layup with the indicated cutout. By changing the orientation of the 45 deg plies with each other, one did not find a change in the bifurcation load or top edge displacement. However, their load bearing capability is reduced. Because the axial stiffness is the same for the two panels, the plots of the top edge load vs the top-edge displacement overlay one another. One notices that the $[90, +45, -45, 0]_s$ panels with the 2×2 in cutouts have the bifurcation load reduced to 81% of the $[0, +45, -45, 90]_s$ panels bifurcation load. The 4×4 in cutout $[90, +45, -45, 0]_s$ panel had its bifurcation load lower than the $[0, +45, -45, 90]_s$. In other words, it can be seen from the linear bifurcation results that the different ply layup did not affect the axial stiffness of the panel. However, the load bearing capability of the panel with the zero degree outside ply was greater.

The panels with the three different ply layups and 2 in² cutouts all had the same top edge displacement of 0.0103 in at their respective collapse loads. The nonlinear collapse load for the $[0, +45, -45, 90]_s$ panel was exactly the same as the $[0, -45, +45, 90]_s$ panel at a load of 215.9 lb/in. The collapse load for the $[90, +45, -45, 0]_s$ panel was a little higher (3.4%) at 223.6 lb/in. Since they are so close to one another, they are represented in Fig. 2 as the same curve for the nonlinear analysis. The zero degree outside ply panels had a collapse lower than the linear bifurcation load. However, the panel with the 90 deg outside ply had a collapse load higher than its respective linear bifurcation.

This item can be explained by considering the stiffness matrix for the panels and the effects a small cutout has on a nonlinear collapse analysis. In the linear bifurcation, the panels had the same axial stiffness. The panels with the zero degree outside plies have a greater bending stiffness and were able to withstand the higher load. When the nonlinear collapse analysis was progressing, the radial displacements and the nonlinearity of the cutout started to come into play. Since the load is applied in the zero degree direction (axial compression), the cutting of this ply orientation by the cutout produces a reduced bending stiffness. Therefore, the panel with the zero degree outside plies allowed the panel to displace radially more than the panels with the 90 deg outside plies. Taking this into account the panels with the 90 deg outside

Presented as Paper 83-0875 at the AIAA/ASME/ASCE/AHS 24th Structures, Structural Dynamics and Materials Conference, Lake Tahoe, Nev., May 2-4, 1983; received Aug. 23, 1983; revision received April 17, 1984. This paper is declared a work of the U.S. Government and therefore is in the public domain.

*Former Graduate Student; presently Engineer, AFSC.

†Professor of Aeronautics and Astronautics, Associate Fellow, AIAA.

plies will have a higher collapse load. Thus, compared to the linear bifurcation analysis, the load bearing capability for the 90 deg outside ply panels will increase in the nonlinear collapse analysis. This is the reason why the nonlinear collapse analysis of the 2x2 in cutout is very close to being the same for both ply orientations and why it falls in between the two linear bifurcations.

The nonlinear collapse load of the 4x4 in cutout was higher than both of the indicated bifurcation loads. This appears to be due to the fact that in the nonlinear collapse analysis the radial displacements along the cutout edges play a greater role in absorbing energy than in the 2x2 in cutout.

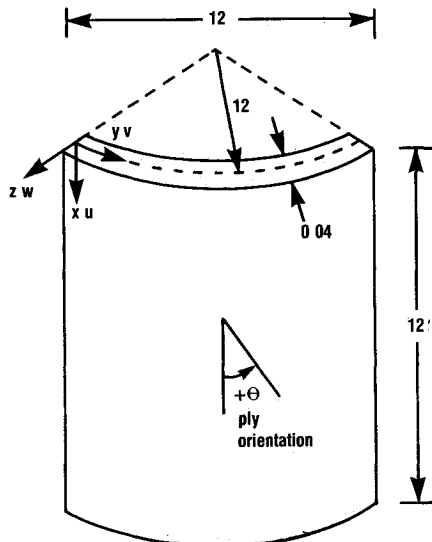


Fig 1 Panel notation

Cutout Size	●[0, +45 -45, 90] _s Panels —[90 +45, -45 0] _s Panel		Collapse Load	Linear Bifurcation
	Ply Layout			
2X2	[0 +45 -45 90] _s		215.9	252.14
2X2	[0, -45, +45, 90] _s		215.9	252.14
2X2	[90 +45 -45 0] _s		223.6	205.0
4X4	[0 +45, -45 90] _s		131.2	113.2
4X4	[0, -45, +45, 90] _s		131.2	113.2
4X4	[90 +45 -45 0] _s			74.32

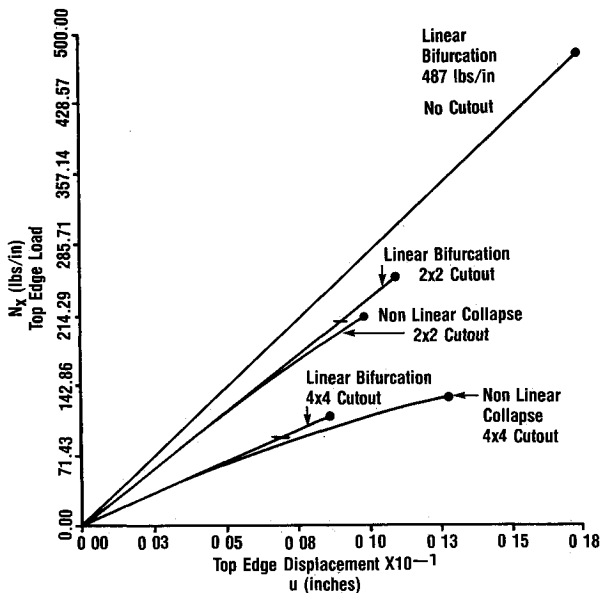


Fig 2 Top edge load vs top edge displacements

and the linear bifurcation of the 4x4 in cutout panel. By having the larger cutout radial displacements along the cutout edges are less constrained in the radial direction and will allow a greater amount of bending. Thus, the panel will be able to absorb more energy (higher collapse load) than the linear bifurcation value and will have a larger top edge displacement.

The w component displacement contours of the panels with a 2x2 in cutout (small cutout) prior to or at the collapse load were given in Ref 8. A difference in the displacement pattern than that experienced by isotropic panels^{2,4} was found; that

Load Level 215.9 lbs/in
Maximum Displacement = .037 inch
Ply Layout [0, +45, -45, 90]_s
Contour Levels Are In 10ths of Maximum Displacement

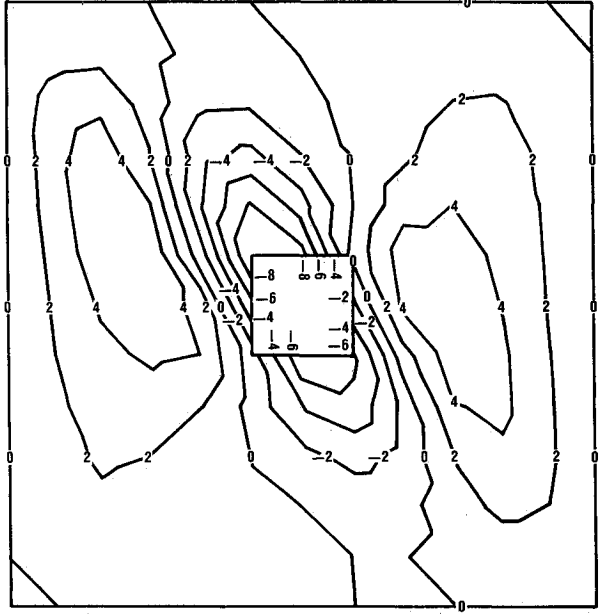


Fig 3 w component displacement contours 2 in cutout.

Load Level 113.2 lbs/in
Maximum Displacement = .084 inch
Ply Layout [0, +45, -45, 90]_s
Contour Levels Are In 10ths of Maximum Displacement

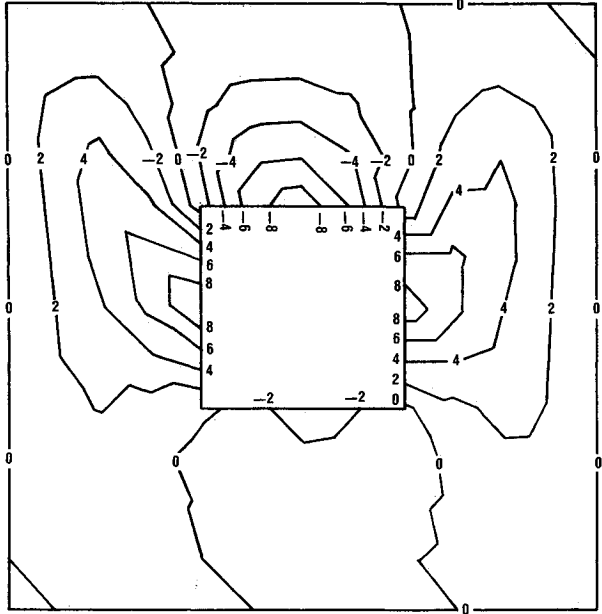


Fig 4 w component displacement contours 4 in cutout

is, at collapse the symmetry about the cutout is lost (see Fig 3). This loss of symmetry is due to the larger radial displacements, hence the larger moments. With the greater radial displacements, the bending stiffness matrix (D matrix) has a greater effect. Therefore, the D_{11} and D_{22} will have an effect on the displacement pattern. A further review of the history of the displacement pattern and the plots of eigenvectors were given in Ref 8.

Figure 4 shows the contours of the radial displacements at collapse load (131.2 lb/in) for the $[0, +45, -45, 90]_s$ panel. The collapse displacement function for the $[0, -45, +45, 90]_s$ panel is the mirror image of that shown in Fig 4. It can be seen that with a 4×4 in cutout the displacement pattern at collapse is more symmetric about the circumferential and longitudinal axis than the panel with a 2×2 in cutout. This is because the larger cutout produces the bending effects earlier and the moment change is more spread out; therefore, a more symmetric displacement pattern. However, the slight amount of nonsymmetry shown at the center of the cutout's vertical edges can be seen to change sides when the ply layup is changed by switching the 45 deg plies. The same phenomenon was experienced with the smaller cutouts. The w component eigenvector contour plots of the 4×4 in cutout panels and the physical interpretation of results were contained in Ref 8.

Conclusions

The following statements and conclusions are based on the analysis presented in this paper.

- 1) Collapse characteristics of composite panels are dependent on the ply layup and the size of the cutouts.
- 2) The 2×2 cutouts (less than 5% of the panel surface area) have a displacement pattern at the collapse load that is different than the larger cutouts. The 2×2 cutouts displacement pattern build symmetrically about the cutout and at the collapse load, snap into the displacement pattern of the eigenvector. The 4×4 cutout had a displacement pattern that stayed fairly symmetric at collapse and was close to the isotropic collapse pattern.
- 3) The load bearing capability of a composite panel is very sensitive to the presence and size of a cutout.

References

- ¹Becker, M. L., Palazotto, A. N., and Khot, N. S., 'Instability of Composite Panels', *Journal of Aircraft*, Vol 18, Sept 1981, pp 739-743.
- ²Tvergaard, V., 'Buckling of Elastic Plastic Cylindrical Panel Under Axial Compression', *International Journal of Solid Structures*, Vol 13, 1977, pp 957-970.
- ³Bauld, N. R. Jr. and Khot, N. S., 'A Numerical and Experimental Investigation of the Buckling Behavior of Composite Panels', *Computer and Structures*, Vol 15, April 1982, pp 393-403.
- ⁴Cervantes, J. A. and Palazotto, A. N., 'Cutout Reinforcement of Stiffened Cylindrical Shells', *Journal of Aircraft*, Vol 16, March 1979, pp 203-208.
- ⁵Starnes, J. H. Jr. and Rouse, M., 'Postbuckling and Failure Characteristics of Selected Flap Rectangular Graphite Epoxy Plates Loaded in Compression', AIAA Paper 81-0543, April 1981.
- ⁶Starnes, J. H. Jr., Knight, N. F. Jr. and Rouse, M., 'Post buckling Behavior of Selected Flat Stiffened Graphite Epoxy Panels Loaded in Compression', AIAA Paper 82-0777, May 1982.
- ⁷Almroth, B. O., Brogan, F. A., and Stanley, G. M., 'Structural Analysis of General Shells Volume II User Instructions for STAGS C 1', Applied Mechanics Laboratory, Lockheed Palo Alto Research Laboratory, Palo Alto, Calif., LMSC D633837, Jan 1981.
- ⁸Janesse, T. C. and Palazotto, A. N., 'Collapse Analysis of Cylindrical Panels With Cutouts', AIAA Paper 83-0875, May 1983.

Flutter Characteristics of High Aspect Ratio Tailless Aircraft

J. R. Banerjee*

University of Wales Institute of Science and Technology
Cardiff, United Kingdom

Introduction

ONE of the examples of high aspect ratio slender wing aircraft is sailplanes. In the next context of their continuing development a tailless design study¹ at Cranfield has claimed an overall performance gain of 10% over conventional types achieved mainly from reduction in the parasite drag. Sailplanes, because of their high aspect ratios and slender wings, are prone to aeroelastic problems such as flutter, even at low speeds. Furthermore the complexity increases in the absence of a tail when the damping in pitch becomes very low. This makes the longitudinal dynamics of the aircraft a formidable problem because it involves an aerodynamic coupling of the rigid body motion with the elastic modes of distortion. Using the basic data for the class of tailless sailplanes given in the design study¹ at Cranfield, this Note investigates such interactions from a selection of extracted results from Ref 2.

The particular class of tailless sailplane under investigation is called the Ricochet^{1,2} and a major section of results is compared with those of an existing class of tailed sailplane the Kestrel-22m. Figure 1 and Table 1 together give the basic details of the two aircraft, whereas Fig 2 shows the structural and aerodynamic properties of their respective wings.

Method of Analysis

The use of generalized coordinates in flutter analysis has been reported earlier by a number of authors^{3,6}. The same method involving normal modes is implemented herein to express mass, stiffness and aerodynamic matrices of the aircraft in terms of the generalized coordinates. The finite element method⁷ is used to obtain the mass, stiffness matrix and the normal modes, whereas strip theory based on Theodorsen expressions³ for unsteady airfoil motion is employed to form the aerodynamic matrix. The flutter matrix is formed by algebraically summing the generalized mass, stiffness, and aerodynamic matrices.

The solution of the flutter determinant is a complex eigenvalue problem because the determinant is primarily a complex function of two unknown variables, the airspeed and the frequency. The method used selects an airspeed and evaluates the real and imaginary parts of the flutter determinant for a range of frequencies. The process is repeated for a range of airspeeds until both the real and imaginary parts of the flutter determinant vanish completely. Once the flutter speed and frequency are established, the corresponding vector, i.e., the flutter mode is found in the classical way by deleting one row of, say, the n th order determinant and solving for $(n-1)$ of the coordinates in terms of the n th.

Results of Computation

The first few wing modes in the symmetric motion obtained from PAFEC⁷ analysis are shown for the Ricochet (four

Received Nov 7 1983; revision received May 7 1984. Copyright © American Institute of Aeronautics and Astronautics, Inc. 1984. All rights reserved.

*Senior Research Associate, Civil Engineering Department, Member AIAA.